The Parton Model

P. Hansson, KTH

November 18, 2004

Abstract

The parton model was introduced in the late 60s by Feynman and Bjorken to address the new data on deep inelastic scattering of electrons on nucleons. The model views the nucleons as made up of point-like constituents and provides a very simple framework for calculating scattering cross sections as well as structure functions for the nucleons. It was very successful in describing a large set of data and also paved the way for particle physicists to later identify the partons with the earlier known quarks of QCD. This report introduces the reader to the parton model and presents the background as well as the most important concepts in deep inelastic scattering.

1 Introduction

One of mankind's oldest questions is "What is the world made of?". Today's particle physics represents mankind's will to continue the search for the answer. Proposed answers has consisted of everything from the four elements (earth, wind, water and fire) to more modern views such as the atom. The periodic table was remarkable in describing chemical properties but because of its apparent structure people believed that the fundamental building blocks of matter was still to be found. Later the nucleus was discovered and subsequently also the nucleons. In the mid 1960s physicists introduced the concept that point-like particles ("quarks") existed inside the proton (Gell-Mann). This idea was mainly based on the effort to describe the rich spectrum of meson and hadron resonances that were discovered during the 1950s, which was interpreted as excited bound states of these point-like constituents. Later, in 1968, new data from SLAC electron scattering experiments hinted that the proton was in fact built up out of point-like particles which physicists at that time called partons. The experiments proved that high-energy electrons have a large probability of scattering with large energy transfers and into large angles. Analogous to Rutherford's famous experiment with the scattering of alpha particles the angular and momentum distributions of the scattered electrons were interpreted as if the proton's charge distribution was localised to a number of small scattering centres. Even though the quark model was successful in describing the variety of baryons there was a period of time when physicists debated whether these quarks were really physical entities and not just non-physical artifacts required by calculations. During this period Feynman introduced the so-called parton model [2] which gave the best description of what the experiments really revealed.

The basic idea of the parton model is that every object with a finite size must have a form factor and therefore experience a dependence on the 4-momentum transfer (Q^2 dependence) from the scattered particle. The experiments at Stanford confirmed the anticipated[1] phenomenon called scale invariance (Bjorken scaling) which proved that scattering of high-energy electrons on the proton where independent of Q^2. This implied that the proton is built up of point-like[1] constituents. The coming years after the Stanford experiments many experimental results indicated that these partons had the quantum numbers from the quark model and as of today it has become clear that the partons in Feynman's parton model can be identified as quarks.

Section 2 gives an introduction to scattering theory which is useful before reading the next section which describes deep inelastic scattering and the structure of nucleons. Section 4 will describe the interpretation of the deep inelastic scattering of electrons on protons and present evidence for Bjorken scaling. A description

[1] It is not known whether they are indeed point-like or if higher resolution experiments will be able to resolve some inner structure. This is indeed interesting but analogous to the atomic case where the inner structure of the nucleus is to first order irrelevant when describing atomic phenomena, the point-like behaviour of the partons is a good approximation.

of the identification of Feynman's partons with the quarks of QCD is given in section 5. The last section gives a conclusion.

2 Introduction to Electromagnetic Scattering

This section will give a very brief explanation of the phenomenology of calculating cross-sections. The goal in this section is to provide the reader with some background and formalism which is necessary to understand the later sections. Also it will show that the basic approach of calculating the large cross-section formulas seen later is simpler than what meets the eye.

2.1 Spin-less Scattering

The most straightforward way of discussing this subject is to start from the very basic level. In this case it is non-relativistic perturbation theory. Assume that we know solutions to the Schrödinger equation $H_0\Psi = E_n\Psi$. The goal is to solve the Schrödinger equation for a particle moving in an interaction potential $V(x,t)$:

$$(H_0 + V(\mathbf{x},t))\Psi = i\frac{\partial\Psi}{\partial t}. \tag{1}$$

We know that any solution can be written as

$$\Psi = \sum_n a_n(t)\phi_n(\mathbf{x})e^{-iE_n t}. \tag{2}$$

We want to find the unknown coefficients $a_n(t)$. We can substitute eq. 2 into eq. 1 and integrate over the volume. If we assume that the particle is in a particular eigenstate i of the unperturbed Hamiltonian a short time before the interaction and that the interaction has ceased a short time later (1st approximation) we can make use of the orthonormality of the solutions and end up with an integral for the coefficient a_f

$$T_{fi} \equiv a_f(\epsilon_t) = -i\int_{-\epsilon_t}^{\epsilon_t} dt \int d^3x \big[\phi_f(\mathbf{x})e^{-iE_f t}\big]^* V(\mathbf{x},t)\big[\phi_i(\mathbf{x})e^{-iE_i t}\big], \tag{3}$$

which can be written as

$$T_{fi} = -i\int d^4x \phi_f^*(x)V(x)\phi_i(x). \tag{4}$$

To obtain a physically meaningful quantity we define the transition probability per unit time as

$$W = \lim_{T\to\infty}\frac{|T_{fi}|^2}{T}. \tag{5}$$

If we integrate over a set of initial (i) and final states (f) we obtain the famous Fermi's golden rule

$$W_{fi} = 2\pi|V_{fi}|^2\rho(E_i). \tag{6}$$

To describe a relativistic electron in an electromagnetic field we must use the Klein-Gordon equation to describe the electron. The Klein-Gordon equation becomes

$$(\partial_\mu\partial^\mu + m^2)\phi = -V\phi \qquad \text{with} \quad V = -ie(\partial_\mu A^\mu + \partial^\mu A_\mu) - e^2A^2. \tag{7}$$

The amplitude (see section 4) is (neglecting the term e^2A^2)

$$T_{fi} = -i\int \phi_f^* ie(\partial_\mu A^\mu + \partial^\mu A_\mu)\phi_i(x)d^4x = ... = -i\int j_\mu^{fi}A^\mu d^4x, \tag{8}$$

where j_μ^{fi} is the electromagnetic current in figure 1,

$$j_\mu^{fi} \equiv -ie(\phi_f^*(\partial_\mu\phi_i) - (\partial^\mu\phi_f^*)\phi_i). \tag{9}$$

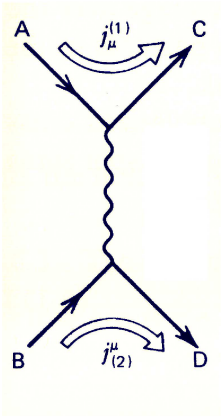

Figure 1: Transition currents in a Feynman diagram.

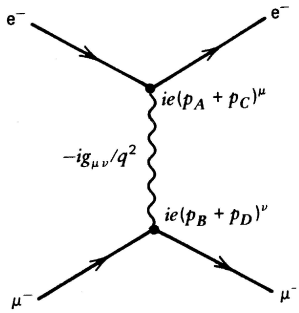

Figure 2: Feynman diagram for spin-less $e^-\mu^- \to e^-\mu^-$.

The electron has four-momenta p_i,p_f and wave solution (free particle) $\phi_i(x) = N_i e^{-ip_i\cdot x}$,

$$j_\mu^{fi} = -eN_iN_f(p_i + p_f)_\mu e^{i(p_i - p_f)\cdot x}. \tag{10}$$

Even though there exists no spin-less leptons, it provides us with a fundamental understanding of scattering of leptons against targets and this will be important for understanding the idea of deep inelastic scattering and all the fancy stuff later.

For example, to obtain the spin-less $e^- \to \mu^-$ scattering we simply need to identify the potential A^μ with the field from the muon. That is, replace A^μ with $-\frac{1}{q^2}j_2^\mu$, where q is the momentum transfer and j_2^μ is the current associated with the muon (fig.1). The scattering amplitude becomes [5]

$$T_{fi} = -iN_AN_BN_CN_D(2\pi)^4\delta^4(p_D + p_C - p_B - p_A)\mathcal{M}, \tag{11}$$

$$-i\mathcal{M} = (ie(p_A + p_C)^\mu)\big(-i\frac{g_{\mu\nu}}{q^2}\big)(ie(p_B + p_D)^\nu), \tag{12}$$

where $\mathcal{M}$ is called the invariant amplitude. The lowest order Feynman diagram is shown in figure 2 where the factor $-i\frac{g_{\mu\nu}}{q^2}$ is called the photon propagator.

We are now in a position to translate the transition amplitude W into a very useful quantity known as the cross-section for a specific process. It is the observable we need to compare the calculations with experiments. The cross-section can be interpreted as the area seen by the incoming particles and be written as

$$d\sigma = \frac{|\mathcal{M}|^2}{F}dQ, \quad \text{(cross section = W / Flux * N(Final states))} \tag{13}$$

where dQ is the Lorentz invariant phase space. The physics resides in the invariant amplitude $\mathcal{M}$.

2.2 Spin and Relativistic Scattering

To move on we need to include relativistic electrons and the fact that electrons are spin particles. The result obtained in section 2.1 therefore needs to be modified. The electrons now have to satisfy the Dirac equation instead of the Klein-Gordon equation. An electron is described by the four-component wave function $\Psi = u(\mathbf{x})e^{-ip\cdot x}$ and the equation to solve is (compare with eq. 7)

$$(\gamma_\mu p^\mu - m)\Psi = \gamma^0 V\Psi, \qquad \gamma^0 V = -e\gamma_\mu A^\mu. \tag{14}$$

Using equation 8 the scattering amplitude is

$$T_{fi} = -i\int j_\mu^{fi} A^\mu d^4x, \qquad j_\mu^{fi} = -e\bar{u}_f\gamma_\mu u_i e^{i(p_f - p_i)\cdot x}. \tag{15}$$

Compare this with equation 9 in section 2.1 for the spin-less electron. In principle we need only to repeat the procedure in section 2.1 to obtain the scattering amplitudes for an electron scattering on a lepton (eg. muon or electron). However, practically this is non-trivial since it involves summing over all spin states. This calculation is simplified when considering the non-relativistic region since the spin direction does not change. This can be understood because the electrons are mostly interacting with their electric field at these energies which cannot flip their spin direction. In the relativistic region one has to carry out the summation over the spins. To obtain the unpolarized[2] cross-section (in the following case for $e^-\mu^- \to e^-\mu^-$) we define the tensors $L_e^{\mu\nu}$ and $L_{\mu\nu}^{muon}$ which separates the sum over the muon and the electron spins

$$L_e^{\mu\nu} = \frac{1}{2}\sum_{spins}[\bar{u}(k')\gamma^\mu u(k)][\bar{u}(k')\gamma^\nu u(k)]^*, \tag{16}$$

and similar for the muon vertex. The invariant amplitude becomes

$$|\bar{\mathcal{M}}|^2 = \frac{e^4}{q^4}L_e^{\mu\nu}L_{\mu\nu}^{muon}. \tag{17}$$

If we switch to the process $e^-e^+ \to \mu^-\mu^+$ by exchanging the appropriate momentum and charges[3] and carry out the tedious summation over the spins we arrive at (using $\alpha = e^2/4\pi$)

$$\frac{d\sigma(e^-e^+ \to \mu^-\mu^+)}{d\Omega} = \frac{\alpha^2}{4s}(1+\cos^2\theta), \quad \sqrt{s}\text{ center-of-mass energy}, \tag{18}$$

where θ is the scattering angle. Figure 3 shows this cross-section measured by the PETRA collaboration (obtained by integrating over $d\Omega$).

2.3 Laboratory Kinematics

This section gives the basics in particle interactions, since the goal of this report is to present the parton model the last part of this section is devoted to the $e^-\mu^- \to e^-\mu^-$ cross-section in the laboratory frame as this is important when studying the structure of the proton. In this frame we assume that the muon from section 2.1 is at rest. The procedure is of course the same, hence we want to determine the invariant amplitude $|\mathcal{M}|^2 = e^4/q^4 L_{\mu\nu}^e L_{muon}^{\mu\nu}$ in this frame. The tensor product can be written[4]

$$L_{\mu\nu}^e L_{muon}^{\mu\nu} = 16M^2EE'\cos^2\frac{\theta}{2} - \frac{q^2}{2M^2}\sin^2\frac{\theta}{2}, \tag{19}$$

where $E(E')$ is the energy of the incoming (outgoing) electron and M is the mass of the muon. Using equation 13 we obtain

$$\frac{d^2\sigma}{dE'd\Omega} = \frac{4\alpha^2(E')^2}{Q^4}\{\cos^2\frac{\theta}{2} + \frac{Q^2}{2M^2}\sin^2\frac{\theta}{2}\}\delta(\mathbf{v} - \frac{Q^2}{2M}). \tag{20}$$

[2]Unpolarized means that no information about the spins is recorded in the experiment.
[3]This is called crossing (Feynman) diagrams.
[4]Neglecting terms proportional to m^2 and M^2[6].

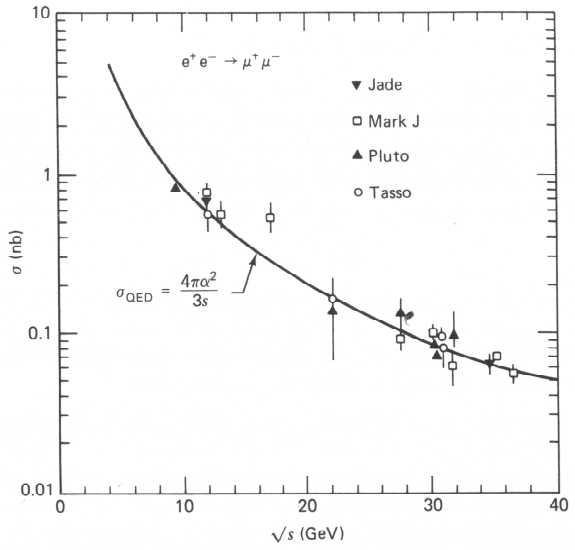

Figure 3: Total cross-section of $e^-e^+ \to \mu^-\mu^+$.

Integrating over dE' we finally obtain

$$\left.\frac{d\sigma}{d\Omega}\right|_{lab} = \left(\frac{\alpha^2}{4E^2\sin^4\frac{\theta}{2}}\right)\frac{E'}{E}\left(\cos^2\frac{\theta}{2} - \frac{q^2}{2M^2}\sin^2\frac{\theta}{2}\right), \tag{21}$$

where $q^2 \simeq -2k\cdot k' \simeq -2EE'(1-\cos\theta) = -4EE'\sin^2\frac{\theta}{2}$. Equation 21 is central in our discussion of deep inelastic scattering and the identification of point-like particles in the proton, discussed in section 3).

3 Deep Inelastic Scattering

This section will give a brief introduction to a large and important field in particle physics, Deep Inelastic Scattering (DIS), deep because the photon penetrates the proton deeply and inelastic because the proton breaks up. The DIS experiments in the late 60s paved the way for understanding the structure of the proton and neutron which was interpreted in the parton model, see section 4. The underlying idea when trying to deduce the structure of composite objects like a hadron is quite simple and straightforward. The simplest experiment you can make is to let a beam of leptons (eg. electrons) scatter on a hadronic target and measure the angle and energy of the scattered lepton. In analogy to atomic physics where the goal is to deduce the wave functions for complex atoms these kind of scattering experiments seek to understand the structure of the constituents of the target.

3.1 Scattering Static Charge Distributions

Very large momentum transfers allows us to resolve smaller objects, the regime $Q^2 \geq 1$ GeV^2 ($Q^2 \equiv -q^2$ is the four-momentum transfer to the target) is referred to as the deep inelastic regime [3]. The resolving power of the probe is approximately $\lambda \sim \sqrt{Q^2}$. Since the scattering in this regime is complicated we begin by considering electron scattering from static charge distributions. Suppose we want to determine the charge distribution of a composite object eg. a charge cloud (figure 4). The procedure to obtain this information is to scatter eg. electrons on this cloud and measure the angular cross-section and compare it with the know cross-section for scattering of a point distribution. As the charge cloud certainly is not a point charge this will give us a form factor ($F(q)$) and the cross-section can be written

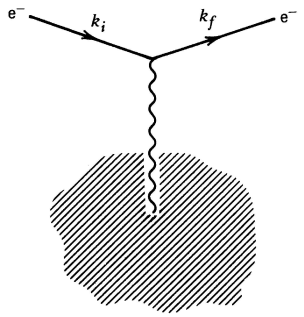

Figure 4: Scattering of a static charge distribution.

$$\frac{d\sigma}{d\Omega} = \left(\frac{d\sigma}{d\Omega}\right)_{point} |F(q)|^2, \tag{22}$$

where q is the four momentum transfer $q = k_i - k_f$. This point cross-section is interesting in a historical point of view, for non-relativistic electrons it corresponds to the famous Rutherford formula which was obtained by scattering alpha particles on nuclei [4]. As the energy of the electrons increases the cross-section will differ from the Rutherford formula, it is now described by the so-called Mott cross-section. For a static, spin-less, spherically symmetric charge distribution the form factor $F(q^2)$ is just the Fourier transform of the charge distribution [5] $\rho(\mathbf{x})$, hence

$$\frac{d\sigma}{d\Omega} = \left(\frac{d\sigma}{d\Omega}\right)_{point} |F(q)|^2 = \frac{(Z\alpha)^2)E^2}{4k^2 \sin^4(\frac{\theta}{2})}\left(1 - v^2 \sin^2(\frac{\theta}{2})\right)|F(q)|^2, \tag{23}$$

$$F(q) = \int_V \rho(\mathbf{x}) e^{i\mathbf{q}\cdot\mathbf{x}} d^3x \quad \text{(Fourier transform)}. \tag{24}$$

The measurement of the cross-section in eq. 23 is a measurement of the form factor and therefore also of the charge distribution. If we expand the form factor (assuming $|-q|$ small), we find

$$\mathbf{F}(\mathbf{q}) = 1 - \frac{1}{6}|\mathbf{q}|^2 < r^2 > +... \tag{25}$$

The small angle scattering is clearly a measurement of the radius of the charge distribution, because the wavelength of the incoming electron is too large to detect the detailed structure of the target [5].

3.2 Elastic Electron-Proton Scattering and Form Factors

When considering scattering of electrons on protons a number of complicated effects must be considered. Many of the results to come are generalizations of the simpler electron-muon scattering, described in section 2 with factors that take into account eg. the mass and the fact that the proton is an extended object compared to the muon. My aim is to provide the reader with the most important features of the theory and to explain their significance. In the previous section we discussed scattering of electrons on a static charge distribution. As stated earlier we must take more effects into consideration, eg. the proton is not static, it will recoil under scattering, the proton's magnetic moment is involved in the scattering and not just the charge and the electron's magnetic moment. These contributions makes the cross section complicated but I will try to give a qualitative description. The starting point is the assumption that the proton is a point charge with Dirac magnetic moment $e/2M$, see figure 5. The cross-section for this is exactly the result in section 2.3 when replacing the muon mass with the proton mass. However, when describing the scattering amplitude T_{fi} it contains an integral over the electron and proton transition currents, described in section 2. The electron and proton transition currents (j^μ) and (J^μ) can be written [6]

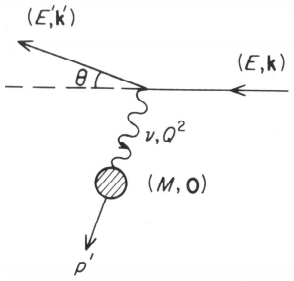

Figure 5: Elastic electron-proton scattering in laboratory frame.

$$j^\mu = -eu(k')\gamma^\mu u(k)e^{i(k'-k)\cdot x}, \tag{26}$$

$$J^\mu = -eu(k')\left[F_1(q^2)\gamma^\mu + \frac{\kappa}{2M}F_2(q^2)i\sigma^{\mu\nu}q_\nu\right]u(p')e^{i(p'-p)\cdot x}, \tag{27}$$

where γ^μ is the vertex factor[5] for the electromagnetic interaction (1st order), $\bar{u}$ and u are spinors representing the outgoing and incoming electrons. We clearly see the differences from a point charge such as the electron[6]. The square brackets in the proton current is a generalisation of an extended structure vertex factor[7]. F_1 and F_2 are independent form factors, κ is the anomalous magnetic moment and σ a spin matrix. Using this current the cross-section becomes

$$\frac{d^2\sigma}{dE'd\Omega} = \frac{4\alpha^2(E')^2}{Q^4}\delta(\mathbf{v} - \frac{Q^2}{2M})\left\{\cos^2\frac{\theta}{2}\left[\frac{G_E^2 + \tau G_M^2}{1+\tau}\right]\cos^2\frac{\theta}{2} + 2\tau G_M^2\sin^2\frac{\theta}{2}\right\}, \tag{28}$$

$$G_E \equiv F_1 + \frac{\kappa q^2}{4M^2}F_2, \tag{29}$$

$$G_M \equiv F_1 + \kappa F_2 \tag{30}$$

with $\tau = \frac{Q^2}{4M^2}$. Carrying out the integration we arrive at the so-called Rosenbluth formula

$$\left.\frac{d\sigma}{d\Omega}\right|_{lab} = \frac{\alpha^2}{4E^2\sin^4\frac{\theta}{2}}\frac{E'}{E}\left(\frac{G_E^2 + \tau G_M^2}{1+\tau}\cos^2\frac{\theta}{2} + 2\tau G_M^2\sin^2\frac{\theta}{2}\right). \tag{31}$$

The form factors G_E and G_M are defined as the electric and magnetic form factors [6]. The form factors can now be determined in experiments (measure θ and q^2). This rather complicated formula for elastic electron-proton scattering reduces to the electron-muon example (eq. 21) if $\kappa = 0$ and $F_1(q^2) = 0$ for all q^2 (ie. if the proton where a point particle [6]). Data for the form factors (figure 6) shows that

$$G_M \approx \left(1 + \frac{Q^2}{0.7\text{GeV}^2}\right)^{-2}, \tag{32}$$

similar for G_E, which causes the elastic cross-section to fall rapidly as Q^2 increases [6]. This dipole behaviour suggests that the proton charge distribution has an exponential shape and Q^2 dependence allows us to measure the proton's charge radius by considering the low Q^2 spectrum of G_E (eq. 25) [5].

[5] 4×4 matrix in spin space.

[6] When $q^2 \to 0$ the form factors must be $F_1(0) = 1$ and $F_2(0) = 1$ since we see a particle of charge e and magnetic moment $(1+\kappa)e/2M$. Corresponding values for the neutron are $F_1(0) = 0$ and $F_2(0) = 1$.

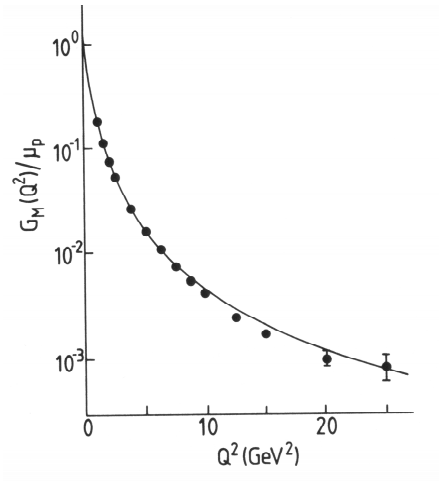

Figure 6: The "dipole fit" of the proton magnetic form factor in eq. 32.

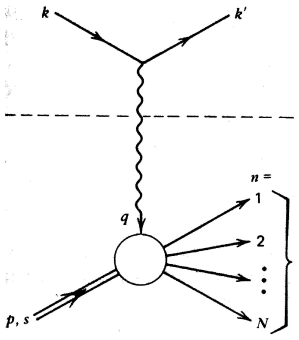

Figure 7: Inelastic electron-proton scattering. Notice the multi-particle final state. The dashed line represents our ignorance to what happens with these states.

3.3 Inelastic Electron-Proton Scattering

Armed with the notation from section 3.2 we now turn over to the more interesting question about the detailed structure of the proton. This is simply done by requiring that the electron loses a large fraction of its energy in the collision. The problem is that when the energy transfer Q^2 becomes larger the proton breaks up, first into resonant baryon states and later (higher Q^2) to complicated multi-particle states as is illustrated in figure 7 [5]. In practice the experiments only need to measure two interaction variables to derive the DIS interaction, two such variables are the electron's energy loss and the angle through which it is scattered. Recalling equations 13 and 17 we now have to reevaluate the technique we used to switch from a muon to a proton target. This was done by replacing the leptonic current j^μ with the hadronic J^μ. Since the final state of the hadron is not a single fermion, it cannot be described by the Dirac spinors u (eq. 15). Therefore we have to replace the muonic tensor in equation 13 with a hadronic tensor $W^{\mu\nu}$ [7]. We can write the cross-section for inelastic electron-proton scattering as

$$\frac{d^2\sigma}{d\Omega dE'} = \frac{\alpha^2}{q^4}\frac{E'}{E}L_e^{\mu\nu}W_{\mu\nu}. \tag{33}$$

The leptonic tensor is unchanged and the most general form of the hadronic tensor must be constructed[7] [5]. For an unpolarized incoming electron the most general form is

$$W^{\mu\nu} = W_1 g^{\mu\nu} + \frac{W_2}{M^2} p^\mu p^\nu + \frac{W_4}{M^2} q^\mu q^\nu + \frac{W_5}{M^2}(p^\mu q^\nu + q^\mu p^\nu). \tag{34}$$

Because of current conservation and the fact that the leptonic tensor $L^e_{\mu\nu}$ is symmetric, only two of the four inelastic structure functions are independent [7]. The hadronic tensor can therefore be expressed in terms of just two independent structure functions W_1 and W_2. Using equations 33 and 16 the cross-section for inclusive[8] inelastic scattering is (laboratory frame)

$$\frac{d^2\sigma}{dE' d\Omega} = \frac{4\alpha^2 (E')^2}{Q^4}\{\cos^2\frac{\theta}{2} W_2(\mathbf{v}, q^2) + 2W_1(\mathbf{v}, q^2)\sin^2\frac{\theta}{2}\}. \tag{35}$$

This is the final result for deep inelastic electron-proton scattering.

In the next section, we will consider how these results can be interpreted and see that our new understanding of scattering and especially deep inelastic scattering is very useful when making conclusion about the structure of the nucleon.

4 Partons

What resides inside the proton? Armed with the earlier sections, we can now interpret the results from deep inelastic scattering.

4.1 Bjorken Scaling

The obvious way to determine if the proton is built up out of point-like particles is to compare the way the cross-section behaves, since it depends heavily on the proton structure functions. Comparing equation 28 for elastic scattering with equation 20 for "point" scattering, we observe that the structure functions W_1^{el} and W_2^{el}

$$W_1^{el}(\mathbf{v}, Q^2) = \frac{Q^2}{4M^2} G_M^2(Q^2)\delta(\mathbf{v} - \frac{Q^2}{2M}), \tag{36}$$

$$W_2^{el}(\mathbf{v}, Q^2) = \frac{G_E^2 + (Q^2/4M^2)G_M^2}{1 + Q^2/4M^2}\delta(\mathbf{v} - \frac{Q^2}{2M}), \tag{37}$$

contains form factors $G_{E,M}(Q^2)$ (see equations 29 and 30). This introduces a mass scale into the structure functions (recall equation 32), the form factors depress the chance of elastic scattering as Q^2 increases and the proton is more likely to break up (sec. 3.2). In contrast, the structure functions for "point" scattering (eq. 20)

$$2mW_1^{point}(\mathbf{v}, Q^2) = \frac{Q^2}{2m\mathbf{v}}\delta(\frac{Q^2}{2m\mathbf{v}} - 1), \tag{38}$$

$$\mathbf{v}W_2^{point}(\mathbf{v}, Q^2) = \delta(\frac{Q^2}{2m\mathbf{v}} - 1) \tag{39}$$

are functions only of the dimensionless variable $\omega = 2q \cdot p/Q^2 = 2M\mathbf{v}/Q^2$ and hence no mass scale is present. The fact that the structure functions at very high energies become less dependent on Q^2 and only dependent on the single variable ω was predicted by Bjorken in the late 60s[9]. He reasoned that if large Q^2 (high-energy) photons resolved point-like constituents in the proton the structure functions would become

$$MW_1(\mathbf{v}, Q^2) \longrightarrow F_1(\omega),$$

[7] The reason for this particular procedure is that we want to parametrize the cross-section without considering the current at the hadronic vertex.

[8] It is called inclusive since we are not measuring the final states of the scattered proton, which hadronize into multi-particle states.

[9] Note that $\mathbf{v}$ and q^2 can be independently varied, since the former only depends on the energy loss of the electron and the latter on the scattering angle.

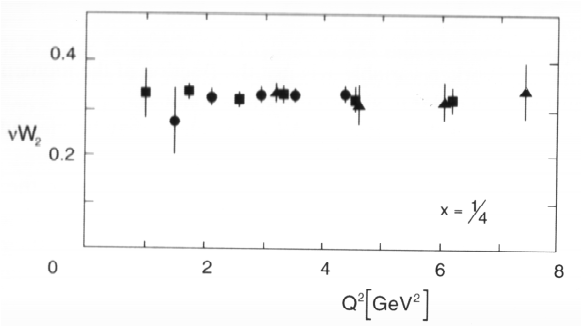

Figure 8: Bjorken scaling for $x = 1/4$.

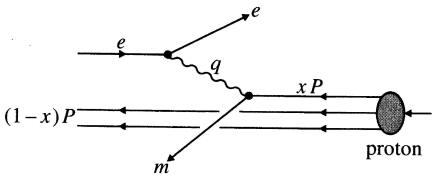

Figure 9: Inelastic electron-proton scattering seen in the infinite-momentum frame.

$$\mathbf{v}W_2(\mathbf{v}, Q^2) \longrightarrow F_2(\omega). \tag{40}$$

This phenomena called Bjorken scaling was experimentally observed in the SLAC experiments in the late 60s, original SLAC data are shown in figure 8. The structure functions $F_{1,2}$ are independent of Q^2 for fixed values of ω. This is the analog to the $\sin^{-4}(\theta/2)$ behaviour of the momentum transfer in the famous Rutherford experiments, which led to the identification of the atomic nuclei. This was the main argument that the photon is interacting with point-like particles, which were named partons, since many people at that time did not believe that quarks were real physical objects.

4.2 Quark Parton Model

The scaling behaviour of the structure functions were quickly understood as scattering on charged point-like particles in the proton. The simplest model that was constructed (which described the data) is called the parton model. The essential idea is that the photon is interacting with free charged point-like particles inside the proton. As in most texts it is simplest to discuss this model in a frame where the proton has a very large momentum $\mathbf{P}$. In this frame (called the infinite momentum frame, see section 6), the constituents of the proton will have mostly collinear momentum with the proton and each parton of charge e_i has a probability $f_i(x)$ to carry a fraction x of the parent proton[10] momentum, see figure 9. Clearly,

$$\sum_i \int x f_i(x) dx = 1, \tag{41}$$

where the sum over i is over all constituents of the proton (uncharged also). The proton (and therefore also the partons) move along the z-axis and the parton (proton) has energy $xE(E)$, longitudinal momentum xp_L (p_L), transversal momentum $p_T = 0$ ($p_T = 0$) and mass $xM(M)$. Assuming that the photon interacts with such point-like partons then,

$$F_1(\omega) = \frac{Q^2}{4m\mathbf{v}x}\delta(1 - \frac{Q^2}{2m\mathbf{v}}) = \frac{1}{2x^2\omega}\delta\big(1 - \frac{1}{x\omega}\big),$$

[10]The proton can be described as $\sum_i \int e_i^2 x f_i(x) dx$.

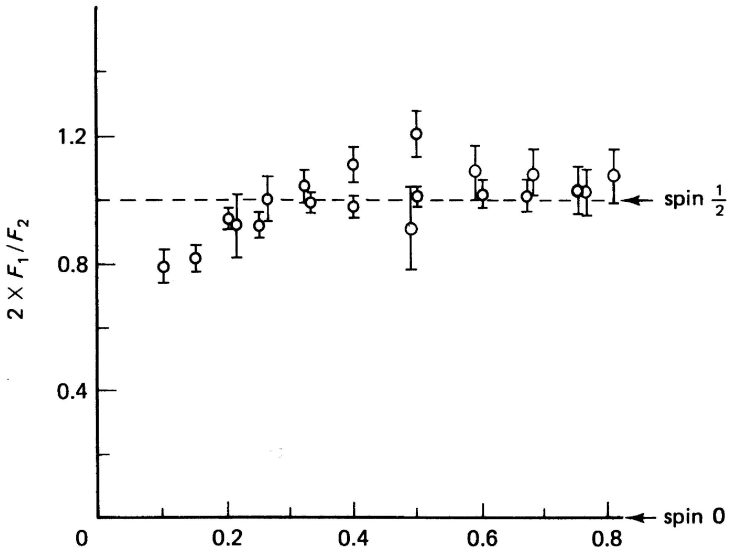

Figure 10: The Callan-Gross relation, which holds well for $x \gtrsim 0.2$.

$$F_1(\omega) = \delta(1 - \frac{Q^2}{2m\mathbf{v}}) = \delta\big(1 - \frac{1}{x\omega}\big) \tag{42}$$

is the structure functions (using equations 40 and 39). The structure function for all the partons is the sum of these (using $\omega = 2M\mathbf{v}/Q^2$ and $\delta(x/a) = a\delta(x)$)

$$F_2(\omega) = \sum_i \int e_i^2 f_i(x) x \delta\big(x - \frac{1}{\omega}\big),$$

$$F_1(\omega) = \frac{\omega}{2} F_2(\omega). \tag{43}$$

The delta function in equation 43 requires that $x = \frac{1}{\omega} = \frac{Q^2}{2M\mathbf{v}}$. This is remarkable, since it tells us that the (virtual) photon must have exactly the correct value of x to be absorbed by a parton with momentum fraction x [5]. It is convenient to rewrite equation 43 in terms of x (called the Bjorken scaling variable) only

$$F_2(x) = \sum_i e_i^2 x f_i(x),$$

$$F_1(x) = \frac{1}{2x} F_2(x). \tag{44}$$

This result, known as the Callan-Gross relation, shown in figure 10, is a cornerstone in the naive parton model. It is a consequence of that the total cross-section for $ep \to eX$ must be divided into two components σ_T and σ_L for transversal and longitudinal polarized (virtual) photons interacting with the proton. For real photons ($q^2 = 0$) it exists only two transversal polarization states, but for a virtual photon ($q^2 \neq 0$) the polarization is not limited to transversal polarization[11]. The ratio between the two polarized cross-sections satisfy

$$\frac{\sigma_L}{\sigma_T} \to 0 \tag{45}$$

for spin-1/2 partons. Consider a head-on collision between a parton and a virtual photon, with the z-axis along $\mathbf{p}$ the conservation of J_z tells us that a spin-0 parton cannot absorb a photon of helicity $\lambda \pm 1$ and

[11] The flux factor is arbitrary for virtual photons [5].

therefore $\sigma_T = 0$. Spin-1/2 partons, on the other hand, can only absorb photons of helicity $\lambda \pm 1$, because they conserve their helicity in high-energy reactions [8] and therefore $\sigma_L = 0$. The experimental data are in very much favour of the spin-1/2 parton case. This relation and the scaling behaviour of the partons showed that the partons were indeed point-like particles with spin-1/2.

However a full QCD treatment of the proton structure including gluons, which are spin-0 particles, leads to a non-zero σ_L. Later high-energy DIS experiments has measured F_L, the so-called longitudinal structure function[9].

5 Quarks

The above results show compelling evidence that the partons in the parton model are point-like fermions. This section will give a brief overview over more evidence that the partons are indeed the quarks of QCD. In the early 70s, the main issue after showing that the partons were fermions was to show that the parton distribution functions predicted the correct mixture of quarks in the nucleon. In this section, the name quark instead of parton will be used to avoid confusion.

5.1 Quark Distribution Functions

The sum in eq. 44 runs over the charged quarks in the proton(or neutron). In the simplest picture, we ignore the presence of charm and heavier quarks, hence

$$F_2^{ep} = x\{(\frac{2}{3})^2[u(x) + \bar{u}(x)] + (\frac{1}{3})^2[d(x) + \bar{d}(x) + s(x) + \bar{s}(x)]\} \tag{46}$$

if $u(x)$ ($\bar{u}(x)$) are the probability distributions of the $u(\bar{u})$ quarks (similar for d and s quarks) and similar for the neutron structure function F_2^{en}. Because of isospin symmetry we can write (using different indices to distinguish between the proton and the neutron)

$$\begin{aligned} u^p(x) &= d^n(x) \equiv u(x), \\ d^p(x) &= d^n(x) \equiv d(x), \\ s^p(x) &\equiv s^n(x) \equiv s(x). \end{aligned} \tag{47}$$

If we treat the proton as a combination of valence quarks and a "sea" of quark anti-quark pairs and assume that the sea is mainly composed of u, d and s quark pairs[12] we can rewrite eq. 46 as

$$F_2^{ep} = x\{\frac{1}{9}[4u_v + d_v] + \frac{4}{3}S\}, \tag{48}$$

$$F_2^{en} = x\{\frac{1}{9}[u_v + 4d_v] + \frac{4}{3}S\}, \tag{49}$$

where the subscript v denote the valence quarks and S is the sea contribution.

It can be shown [5] that if the cross-section behaves as a constant when $x \to 0, v \to \infty$ for fixed Q^2, i.e.,

$$f_i(x) = \frac{1}{x} \tag{50}$$

and this means that the growth of quarks is logarithmic at small x. The three valence quarks are therefore drowned by this low-momentum debris and consequently

$$\frac{F_2^{en}(x)}{F_2^{e}p(x)} \to 1 \quad \text{as } x \to 0. \tag{51}$$

[12]The contribution due to heavy quarks c, b and t pairs are suppressed by their masses. Also, the sea S is assumed to contain equal number of $u\bar{u}$, $d\bar{d}$ and $s\bar{s}$ pairs.

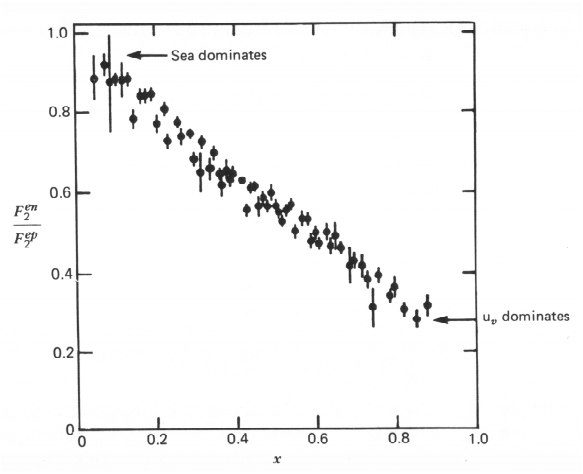

Figure 11: Deep inelastic scattering data of the ratio F_2^{en}/F_2^{ep}.

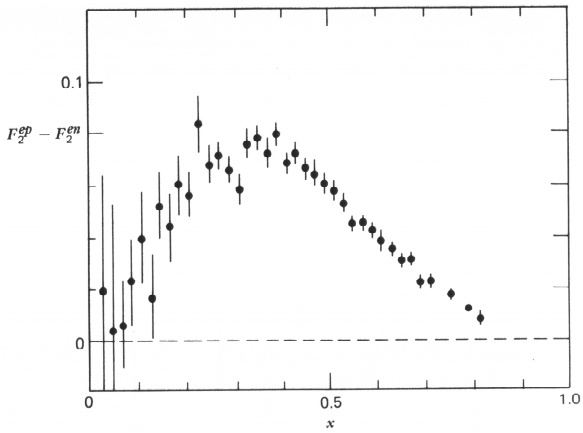

Figure 12: Deep inelastic scattering data of the difference $F_2^{ep} - F_2^{en}$.

On the other hand, when $x \to 1$ the valence quarks carry most of the momentum and the ratio is expected to become

$$\frac{F_2^{en}(x)}{F_2^{e}p(x)} \to \frac{u_v + 4d_v}{4u_v + d_v} \quad \text{as } x \to 1. \tag{52}$$

For the proton the probability function $u_v \gg d_v$ and the ratio in eq. 52 tends to 1/4. The experimental evidence is shown in figure 11.

What does the actual structure functions $F_2^{ep}(x)$ look like?[13] If the electron scattered off a free quark carrying a fraction x of the proton's momentum, the structure function would be a delta function $F_2^{ep}(x) \approx x\delta(1/3 - x)$ if $m_u = m_d$. In reality, the quarks are not completely free and especially the mass of a quark inside a hadron is not well defined and it is useful to consider the mass as a continuous variable. The structure function is therefore smeared around $1/3x$. Also the slow debris (eq. 50) is expected to enlarge $F_2^{ep}(x)$ at low x. There is a way of looking at the valence quark distribution without the sea contribution, that is $F_2^{ep}(x) - F_2^{en}(x) = x1/3[u_v - d_v]$ which should peak around 1/3. Such a measurement is shown in figure 12.

[13]Remember that $F_1(x) = \frac{1}{2x}F_2(x)$.

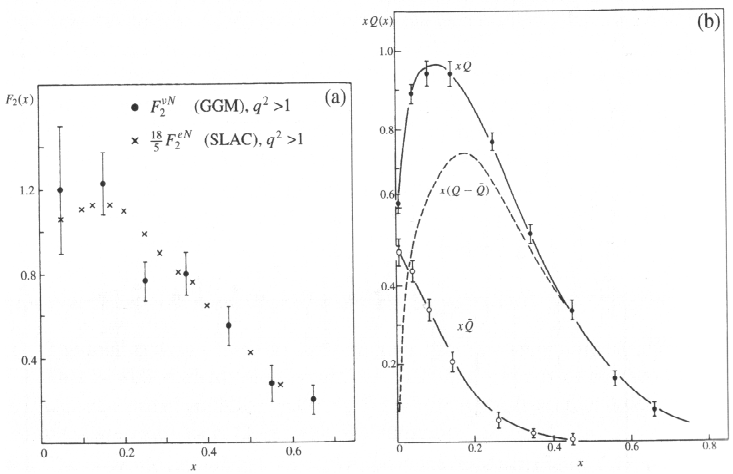

Figure 13: (a) Data from CERN on $F_2^{\nu N}(x)$ compared with SLAC data on $F_2^{eN}(x)$, (b) momentum distributions of quarks and anti-quarks.

5.2 Quark, Anti-Quarks and Gluons

The most compelling arguments to identify the partons with quarks of QCD is the comparison of deep inelastic scattering events with electrons and neutrinos. From a similar discussion as in section 5.1, a nucleon target with same number of u and d quarks has a structure function

$$F_2^{eN} = x\frac{5}{18}(u(x) + \bar{u} + d(x) + \bar{d}) + \frac{1}{9}(s(x) + \bar{s}). \tag{53}$$

One can define similar structure functions for neutrino and anti-neutrino scattering (through W exchange)

$$F_2^{\nu N} = u(x) + \bar{u} + d(x) + \bar{d}. \tag{54}$$

For simplicity this is done for $x \geqslant 0.3$ where the sea contribution is negligible [4], comparing eq. 53 with eq. 54 $F_2^{eN} = 5/18F_2^{\nu N}$. The data supporting this prediction is shown in figure 13.

The quarks of QCD are known to interact via exchange of bosons, the gluons. How can we find evidence for the gluons? Since the quarks are continuously interacting via these particles it should be possible that these particles also carry some fraction of the parent proton's momentum. In the simplest model where one neglects all other but the u and d quark contributions eq. 46 can be written as

$$F_2^{ep} = x\{(\frac{2}{3})^2[u(x) + \bar{u}(x)] + (\frac{1}{3})^2[d(x) + \bar{d}(x)]\}. \tag{55}$$

The data clearly show that $u(x) \neq 2d(x)$ but the average momentum carried by up type quarks is twice of the momentum carried by d-quarks,

$$\int_0^1 xu(x)dx = 2\int_0^1 xd(x)dx. \tag{56}$$

Combining equation 56 and 55

$$\int_0^1 xd(x)dx = \int_0^1 F_2(x)dx. \tag{57}$$

So a measurement of the area under $F_2(x)$ is a measurement of how large momentum fraction the d quarks carry. Using fig. 14 we estimate

$$\int_0^1 F_2(x)dx = \int_0^1 xd(x)dx = 0.18 \quad \Rightarrow \quad \int_0^1 xu(x)dx = 0.36. \tag{58}$$

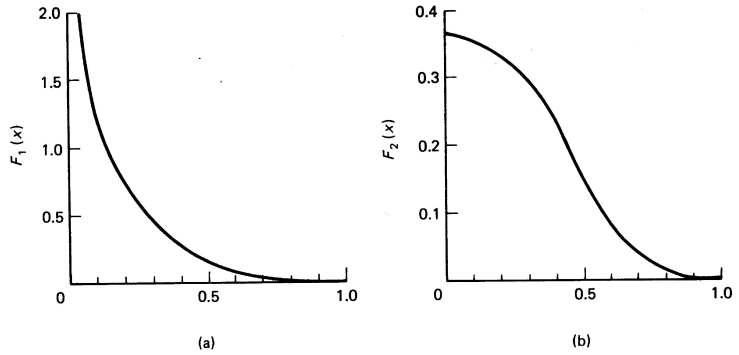

Figure 14: Data on (a) $F_1(x)$ and (b) $F_2(x)$.

The average momentum carried by quarks are only $18\%+36\% = 54\%$ of the total momentum of the proton. Since the photon only probes the charged particles, neutral particles do not contribute to the cross-section and it seems that about 50% of the proton's momentum is carried by these neutral particles. Thus, deep inelastic scattering also provides evidence of the exchange particles in the quark interaction.

5.3 Scaling Violations

The scaling behaviour of the structure function is well known to be an evidence of scattering against point-like particles. This behaviour can be understood when comparing the parton model result with lower Q^2 regions as the analogy of Rutherford scattering. More generally, the dimensionless variable $\mathbf{v}W_2$ (eq. 39) for elastic scattering is only dependent on one variable (involves typically $\delta(x-1)$) and is multiplied with a dynamic form factor (remember sec. 3.1). This factor could correspond to the target having a finite size and therefore can be excited and such processes typically involve some additional Q^2 dependence. This form factor can be written as $(1+Q^2/\Lambda^2)^{-N}$ (see for example eq. 32) where the parameter Λ is a measure of how point-like the object is, more point-like gives larger Λ. A muon target which appears to be completely structureless has $\Lambda \to \infty$ and hence is controlled by a delta function constraint on the kinematics. A muonic target is therefore said to be scale invariant. Switching now to electrons scattering on protons the proton seems to be point-like as long as $Q^2 \ll \Lambda^2$. When $Q^2 \gg \Lambda^2$ the structure of the proton is revealed and the form factor kills the cross-section with increasing Q^2. The same pattern is followed in electron-nucleus scattering where the cross-section is first dominated by the elastic scattering from the nucleus and nuclear excitations. At even higher energies (when $Q^2 \gg \Lambda^2$) the structure function reveals the finite size of the nucleus killing the elastic cross-section and the elastic scattering on the constituents of the nucleus dominates the cross-section revealing the point-like behaviour of the proton and the neutron.

These "scaling" can be understood by the above discussion, but experiments during the early years of deep inelastic scattering noticed another scaling behaviour which did not exactly follow this pattern. Bjorken scaling was a well-known fact, but the experiments showed that it was only an approximate scale invariance since the scaling was dependent on the Bjorken variable x. Figure 15 show the experimental evidence for the scaling violation. The data shows that the structure function in reality also has a logarithmic dependence on Q^2, which was not anticipated by the parton model. It was here that QCD had its first great success in predicting the correct scale behaviour for the structure function.

Qualitatively the scaling can be understood as follows:

- $x > 0.2$: The valence quarks dominate this region and it can be shown that the process where the valence quark emits a gluon before interacting with the photon is increasingly important in this regime. As the emitted gluon carries some of the initial quark momentum the quark distributions shrink towards smaller x as Q^2 increases even more. This describes the decrease of the structure function for larger Q^2.

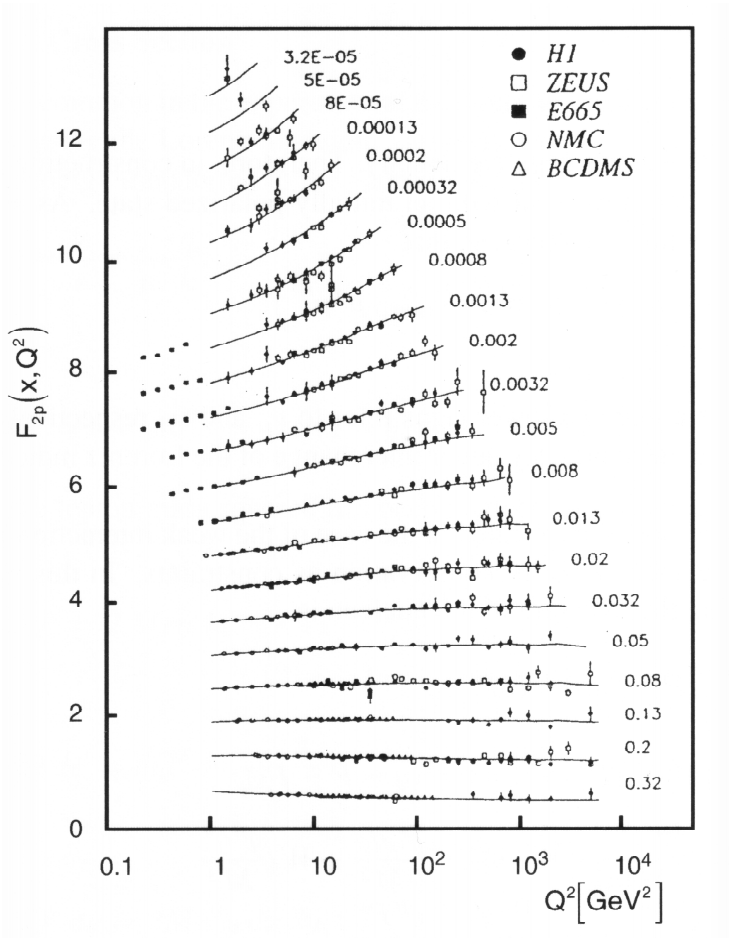

Figure 15: Scaling violation for different x values.

- $x \to 0$: When Q^2 increases the emission of gluons is more probable which causes a slight increase of the structure function with higher Q^2. This increase is seen at low x, where the sea quark contribution is more important.

6 Conclusions

The parton model introduced by Feynman was the first model that could describe the data from the DIS experiments in the late 60s. With the advent of higher energy DIS interactions, modifications to the parton model in terms of gluon distributions were made. The implication of the parton model is huge, as of today the parton model is one of the fundamental ingredients necessary in describing particle interactions. Typically most Monte Carlo generators use proton density functions (PDF's) to parametrize the quark and gluon distributions of the parton model according to perturbative QCD. Any deviation discovered in today's (e.g. the Tevatron) or future high-energy particle colliders like the LHC would be of profound importance, signaling new physics or possible quark substructure.

Appendix

Infinite Momentum Frame

When defining the variables in section 4.2 (for example the partons fractional momentum xp) we actually need to work in the infinite momentum frame. This procedure is also known as the impulse approximation. The requirements for our calculations to be justified are that during the time the photon interacts with the parton we can neglect parton parton interactions and that final state interactions can be ignored. In nuclear physics, the partons are nucleons and a nucleon is being struck so hard that the nucleus shatters and the final state is indeed absent. In the parton model the nucleons are now quarks of QCD and satisfy color confinement. This means that a quark cannot completely be removed from the nucleon and requires that we need another assumption, that the final state interactions between the quarks is carried out over a larger space-time distance than the photon interaction[14]. The most widely used picture for this is that the quarks are connected to one another with a color confining elastic band. The assumption is then that during the time the photon interacts with a parton it can be regarded as quasi-free and the effects of the elastic band arises later. This frame is also known as the Breit frame or Brick frame.

References

[1] J.D. Bjorken, *Proceedings 3rd International Conference on Electron and Photon Interactions, Stanford, (1967), Phys. Rev. 185 (1969) 1975 (with E.A. Paschos)*

[2] R.P. Feynman, *Phys. Rev. Lett. 23 (1969) 1415*

[3] Anthony W. Thomas, Wolfram Weise, *The Structure of the Nucleon*

[4] B.R. Martin, G.Shaw, *Particle Physics*

[5] F. Halzen, A.D. Martin, *Quarks and leptons*

[6] F.E. Close, *An Introduction to Quarks and Partons*

[7] D. Griffiths, *Introduction to Elementary Particles*

[8] D.H. Perkins, *Introduction to High Energy Physics*

[9] H1 Collaboration, *Determination of the Longitudinal Proton Structure Function $F_L(x, Q^2)$ at Low x, ISSN 0418-9833, Nov. 1996*

[14] Of the order of the proton size.